

Synthesis and Characterization of PMMA Polymer/Clay Nanocomposites for Removal of Dyes

E.J. SARAVANA SUNDARAM and P. DHARMALINGAM*

PG and Research Department of Chemistry, Urumu Dhanalakshmi College, Tiruchirappalli-620019, India

*Corresponding author: E-mail: dharmalingamudc@gmail.com

Received: 11 April 2019;

Accepted: 7 July 2019;

Published online: 28 September 2019;

AJC-19591

The adsorbent polymer/clay nanocomposites were prepared by *in situ* emulsion polymerization method. The prepared adsorbent was characterized using FT-IR, XRD, TGA and the surface morphology was analyzed using FE-SEM. The prepared polymer/clay nanocomposite was used for the removal of malachite green and amido black 10B. The effects of initial pH, adsorbent dosage, initial metal ion concentration, contact time and thermodynamic studies on the malachite green and amido black 10B adsorption were studied. The adsorption isotherm parameters of the adsorption process were determined by using Langmuir, Freundlich and Temkin adsorption isotherm equations. The kinetic parameters were predicted with Lagergren's pseudo-first order and pseudo-second order equations. The effect of temperature of the adsorption process was demonstrated by using the thermodynamic parameters. The maximum adsorption capacity of malachite green and amido black 10B onto polymer/clay nanocomposites was found at pH 7 and 2. Adsorption of malachite green and amido black 10B onto polymer/clay nanocomposites followed the Langmuir adsorption isotherm and it follows pseudo-second order rate constant equation. The thermodynamic parameters, such as ΔH° , ΔS° and ΔG° were also determined which suggested that the studied adsorption process was an endothermic reaction.

Keywords: Synthesis, PMMA polymer, Nanocomposites, Removal, Dyes.

INTRODUCTION

Industries such as textile, dyeing, tannery, paper, paints, plastics, *etc.* are the source for dye effluents which are highly toxic, carcinogenic, and allergenic on exposed organisms [1]. About 10-50 % of dyes (reactive, acidic, basic and metal complex) remain in the wastewater [2]. There are 3000 types of dyes available among which the cationic dyes are much more toxic than the anionic dyes [3]. A wide range of conventional methods such as chemical oxidation, precipitation, coagulation, flocculation, ion exchange, photodegradation, reverse osmosis and biological treatment have been investigated for the removal of dyes [4,5]. Due to some limitations the above mentioned methods were suffered in complete removal of color from the wastewater. In addition to this, the dyes present in wastewater are characterized by high salt content and low biodegradable potential which makes the conventional wastewater treatment processes very difficult [6]. Adsorption is a superior and effective method for the removal of dyes in terms of simplicity of design, low initial cost of operation, ease of operation, local availability,

and sensitivity to toxic substances [7-9]. Various adsorbents used for color removal, includes activated carbon, agricultural wastes, zeolites, clay minerals, polymeric materials, *etc.* [10-12]. Activated carbon is one of the most commonly used adsorbent for water purification due to its high surface area, porous structure and thermal stability, and has several disadvantages. They are expensive, fine powdered and produces solid wastes. The regeneration of activated carbon by chemical and thermal processes is expensive and very difficult. A number of low cost novel adsorbents such as fly ash [13,14], clay mineral [15], *etc.* were introduced.

Clays is a low-cost adsorbent and easily available [16]. They are environmental friendly materials with high surface area, structural properties, chemical stability and mechanical stability [17]. Smectite group clays and kaolinite group clays are the type of clays used for the preparation of nano-adsorbents. The smectite group clays are composed of hydrated sodium calcium aluminum silicate, a family of non-metallic clays, which includes montmorillonite, bentonite, *etc.* as their group members [18]. Due to the negative charge of clay surface that

can attract and hold the cations of several substances such as cationic dyes, heavy metals, *etc.* [19]. In order to improve the adsorption capacity of clays, it can be activated and modified [20]. It can also be applied in the fields such as polymer nanocomposites [21-23], catalysts [24], photochemical reaction [25], *etc.* The separation of suspended clay materials from the aqueous solution is difficult, so there is a need to bind the clay with polymer matrix for making the separation more comfortable [26].

Now-a-days, the nanoparticles play an important role by modifying their surface functionality [27]. By mixing the clay with polymer matrix results in a class of new micro-composite and nanocomposite materials. The nanocomposites also exhibit excellent physical, thermal and mechanical properties. Polymer/clay nanocomposites are of great interest in water purification because of their structural or functional behaviour [28,29]. By comparing it with pure polymer, the polymer nanocomposites enhance excellent properties such as reduced thermal expansion, reduced gas permeability, good ionic conductivity, mechanical strength, flame retardancy, *etc.* [30-32]. Polymer/clay nanocomposites is not only low-cost but also effective for the removal of pollutants from the wastewater.

Present study focuses on the preparation of polymer/clay nanocomposites *via in situ* emulsion polymerization using methyl methacrylate as monomer. The prepared nanocomposite was characterized using FT-IR, XRD, FE-SEM and TGA. A batch experiments were carried out to investigate the adsorption capacity, equilibrium isotherms, kinetics and thermodynamics of the prepared nanocomposites in aqueous solution.

EXPERIMENTAL

Analytical grade reagents were used for the adsorption study. A 1000 mg/L of stock solution was prepared. Reactive dyes used in this study are malachite green and amido black 10B from Aldrich Chemicals, USA. Bentonite was used as an adsorbent and supplied by S.D. Fine-Chem Limited Mumbai, India. Tetrabutylammonium bromide was received from SRL, Mumbai, India.

Preparation of organoclay: The organic clay was prepared *via* ion-exchange reaction. The clay about 10 g was dispersed in deionized water at room temperature followed by mixing for 1 h at 25 °C. Tetrabutylammonium bromide (10 g) was dissolved in water at 25 °C and slowly added to clay suspension of about 800 mL. The suspension was mixed at 25 °C for 24 h and filtered using disc filter funnel. The modified clay was washed several times with redistilled water. Until no bromide ion was detected by using AgNO₃ solution. The obtained organoclay was dried at 80 °C for 12 h.

Preparation of clay/polymer nanocomposites by *in situ* emulsion polymerization: Prepared organoclay was dispersed in water and mixed with 10 % methyl methacrylate. The suspension was then stirred for 2 h at 80 °C. Potassium per sulfate (0.0265 g) as initiator was then added to initiate the polymerization reaction and then the surfactant as sodium luryl sulfate of about 0.53 g was added and refluxed for 4 h at the same temperature. The polymer was then precipitated with methanol and then filtered using disk funnel. It was then allowed to dry using vacuum oven for about 30 min at 170 °C [33].

The surface functional groups of the polymer/clay nanocomposites were estimated by FT-IR spectroscopy (FT-IR-2000, Perkin Elmer) analysis. FT-IR spectra of the sample were recorded in the range of 4000-400 cm⁻¹. External morphology of nanocomposite was observed and characterized by field emission scanning electron microscopy (FE-SEM), obtaining magnified three-dimensional-like images of their surfaces. X-ray powder diffraction (XRD) is an analytical technique primarily used for phase identification of a crystalline material and can provide information on unit cell dimensions.

Thermogravimetric (TGA) analysis of the composite and the neat polymer were analyzed using 2950 TGA V5.4A thermal analyzer under nitrogen flow at the heating rate of 20 °C/min. The zero-point charge (pHzpc) and surface functional groups of clay/polymer nanocomposites were characterized according to Boehm titration method.

Adsorption experiments

Equilibrium experiments: Adsorption equilibrium is used to describe the experimental adsorption data. The importance of equilibrium adsorption is obtaining the "best-fit" isotherm, which is more significant and the detailed isotherm descriptions are required for the adsorption system design.

The amount of adsorbed adsorbate at equilibrium, q_e (mg/g) was calculated by

$$q_e = \frac{(C_o - C_e)}{W} V$$

where C_o and C_e (mg/L) are the liquid phase initial and equilibrium concentrations of adsorbate respectively. V is the volume of the solution (L) and W is the mass of dry adsorbent used (g).

Kinetic studies: The kinetic experiments are used to investigate the mechanism of adsorption and rate controlling step. The amount of adsorption of adsorbate solution was calculated at various time intervals. The amount of adsorption (q_t) at time 't' was calculated by the following equation:

$$q_t = \frac{(C_o - C_t)}{W} V$$

where C_o and C_t (mg/L) are the liquid-phase concentrations of the adsorbate at initial and time t , respectively. V is the volume of the solution (L) and W is the mass of dry adsorbent used (g).

Thermodynamic studies: Thermodynamic experiments were done at various temperatures and the thermodynamic parameters of the adsorption process were determined from the experimental data.

RESULTS AND DISCUSSION

The FT-IR spectra of modified TBAB polymer/clay nanocomposites is analyzed in the range of 400-4000 cm⁻¹. Fig 1a confirms the presence of OH at 1462 and 1631 cm⁻¹ adsorption bands, CH₂ and CH₃ at 2911 and 2842 cm⁻¹, silicate structure [Si-O-Fe], [SiO] at 534-465 cm⁻¹, and dioctahedral smectite with [Al, Al-OH] at 3698 cm⁻¹, stretching and bending bands. Powder XRD patterns of the prepared clay/polymer nanocomposites were recorded at 0.1° increments at 10 sec per point. The obtained peak in the XRD patterns of adsorbent was compared with Joint Committee on Powder Diffraction Standards (JCPDS)

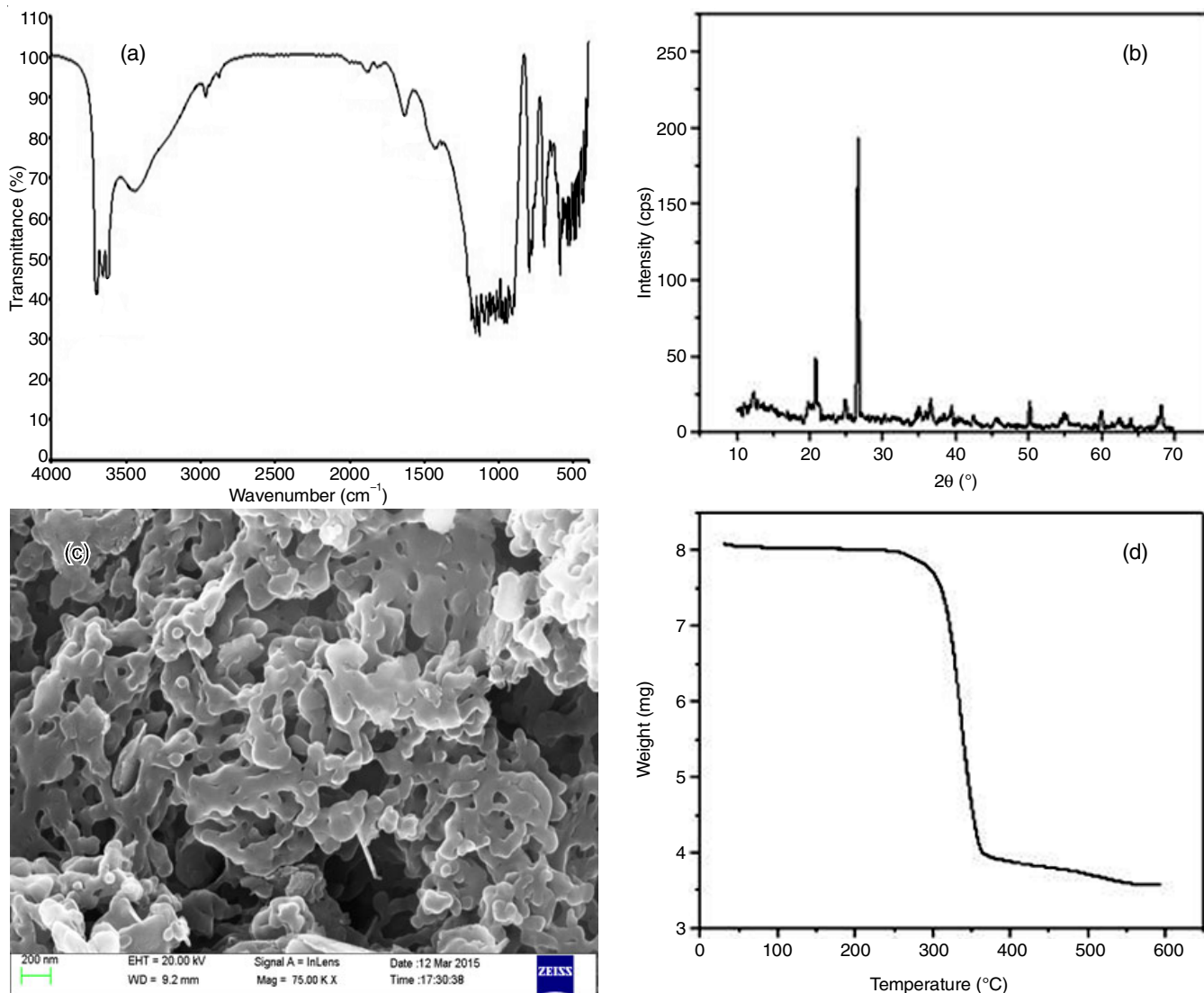


Fig. 1. Characterization of polymer/clay nanocomposites (a) Fourier transform infrared spectroscopy, (b) XRD pattern, (c) FE-SEM analysis and (d) Thermogravimetric analysis (TGA) for polymer/clay nanocomposites

data. The XRD analysis (Fig 1b) showed that bentonite consists of montmorillonite, quartz, feldspar and calcite. It was used directly for adsorption experiments without any treatment.

The FE-SEM image in Fig 1c shows the porous structure, size distribution and shape of the nanoparticles which have a layered structure. It was observed that the adsorbent have rough texture with heterogeneous surface and a variety of randomly distributed pore size. This figure shows the good arrangement of nanoparticles over the surface of clay/polymer. The size distribution of these nano particles was approximately 40 nm and the shape of nanoparticles were cubic in nature.

Thermogravimetric analysis (TGA) was analyzed between 20 and 600 °C showed in Fig. 1d and follows the weight loss of adsorbent. These transformations are due to the removal of adsorbed and interlayer water from the clay minerals. The zero-point charge and the surface functionality of adsorbent were also evaluated. It was found that the zero-point charge plays an important role in the whole process which lies around pH 6.62. The surface functionality analysis shows the adsorbent contained more basic functional groups (0.317) on their surface when compared to the acidic functional groups (0.116).

Effect of pH on adsorption: The pH of the dye solutions plays an important role in the whole adsorption process, particularly on the adsorption capacity. This also has an influence on the surface charge of adsorbent, degree of ionization of materials that is present in the solution and dissociation of functional groups. The pH of the solution was controlled by the addition of HCl and NaOH. In general, the anions are favourably adsorbed by the adsorbent at lower pH due to the presence of H⁺ ions, and the cations at higher pH due to the negatively charged surface sites [34,35]. The pH of the dye solution affects the structural stability and also their colour intensity. Adsorption of dyes onto the adsorbents was studied at different pH varying from 2 to 10 for the prepared adsorbents. It was found that there is no significant change for malachite green with varying pH the maximum adsorption occurred at pH 7 for malachite green, and at pH 2 for amido black 10B. The maximum percentage adsorption of malachite green was (92.25 %) and amido black 10B (62.74 %). Therefore, all further experiments were carried out in distilled water and required pH of each dyes.

Effect of adsorbent dosage: The effect of adsorbent dosage was carried out by varying the clay/polymer dosage from 0.01

to 1.0 g/10 mL. It was found that the percentage adsorption increased with the increase in the adsorbent dosage. The maximum malachite green and amido black 10B removal efficiency of 98.81 and 90.02 % was observed at the dosage of 0.1 g/10 mL.

Effect of initial dyes concentration: The effect of initial dye concentration was studied by varying the initial malachite green, amido black 10B concentrations from 5 mg/L to 1000 mg/L for clay/polymer. The percentage adsorption decreased with the increase in the initial concentration dye is shown in Fig. 2a. At lower concentration, the ratio of initial number of dye molecules to the adsorbent available surface area is low, however for higher concentration the available sites become

fewer and the percentage removal is dependent upon the initial concentration [36].

Adsorption equilibrium isotherms: Equilibrium isotherm model equations such as Langmuir, Freundlich and Temkin isotherms are used to describe experimental adsorption data. It is important to find the best-fit isotherm to evaluate the efficacy of the prepared adsorbent to develop suitable industrial adsorption system designs.

Langmuir adsorption isotherm: The Langmuir equation is probably the best known and widely used for adsorption isotherm and it is based upon the assumption of monolayer adsorption on to a surface containing a finite number of adsor-

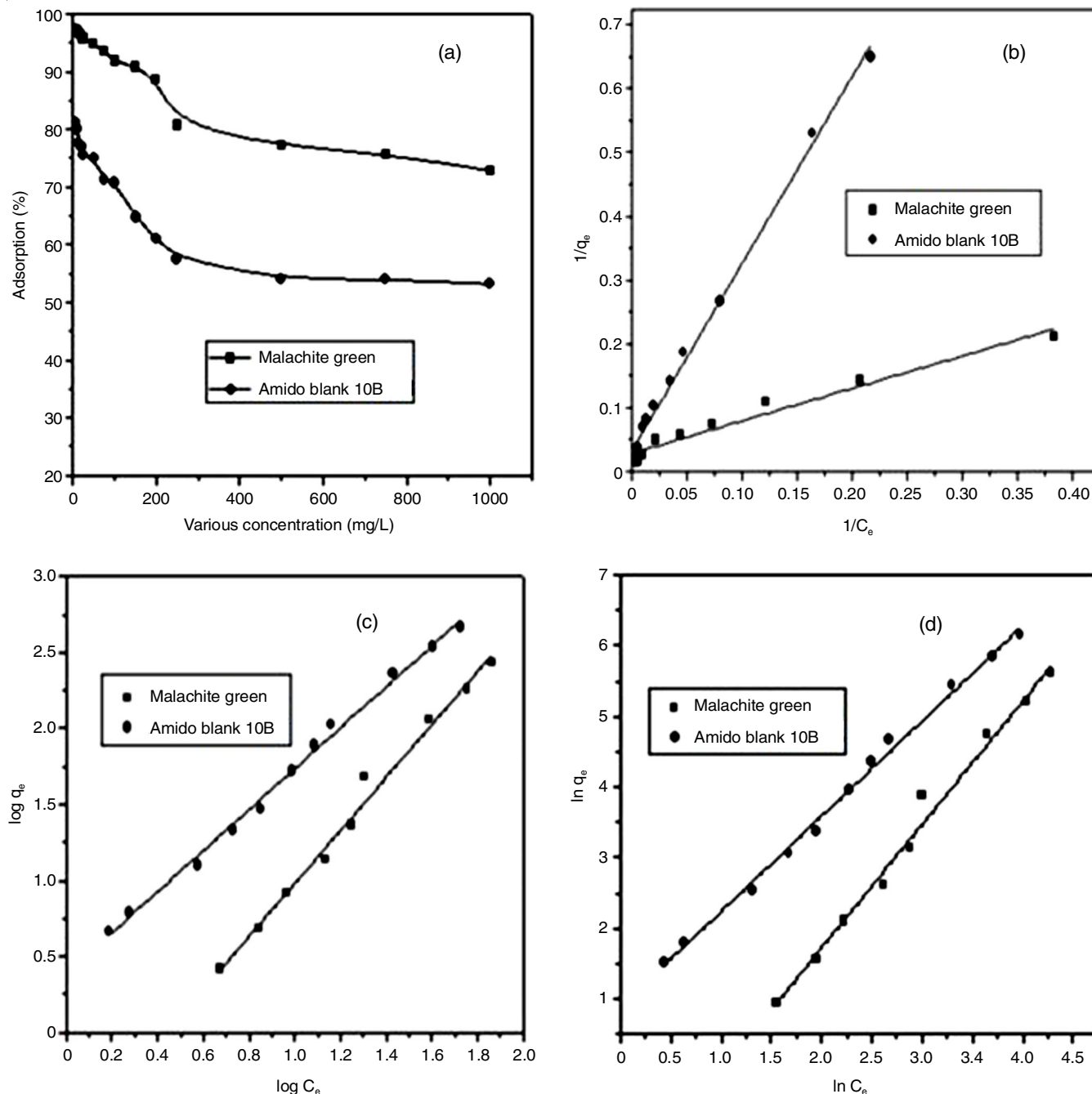


Fig. 2. Plots of adsorption isotherm for adsorption of malachite green and amido black 10B onto clay/polymer nanocomposites at different initial dye concentration. (a) Percentage adsorption, (b) Langmuir adsorption isotherm, (c) Freundlich adsorption isotherm, (d) Temkin adsorption isotherm

ption sites of uniform energies of adsorption [37,38]. It is represented as follows:

$$q_e = \frac{K_L C_e}{1 + q_m K_L C_e} \quad (1)$$

A linear form of this expression is

$$\frac{1}{q_e} = \frac{1}{q_m K_L C_e} + \frac{1}{q_m} \quad (2)$$

where q_e (mg/g) and C_e (mg/L) is the amount of adsorbate adsorbed per unit mass of adsorbent, concentration of unadsorbed adsorbate; K_L (L/g) is the Langmuir constant and K_L/q_m gives the theoretical monolayer saturation capacity, q_m (mg/g). A plot of C_e/q_e versus C_e gives a straight line with slope q_m/K_L and intercepts $1/K_L$.

The Langmuir isotherm can also be expressed in terms of dimensionless constant called separation factor [37,39], which is defined by the following equation:

$$R_L = \frac{1}{1 + K_L C_e} \quad (3)$$

where R_L is the equilibrium parameter, C_e (mg/L) is the initial adsorbate concentration, R_L indicates the shape of isotherms to be either favourable ($0 < R_L < 1$), unfavourable ($R_L > 1$), irreversible ($R_L = 0$) and linear ($R_L = 1$).

Freundlich adsorption isotherm: The Freundlich adsorption isotherm model can be applied to the non-ideal adsorption on heterogeneous surfaces and also for the multi-layer adsorption [40,41], which can be expressed by the following equation:

$$q_e = K_F C_e^{1/n} \quad (4)$$

The linear form of the above equation becomes as

$$\log q_e = \log K_F + \frac{1}{n} \log C_e \quad (5)$$

where K_F (L/g) is the Freundlich constant and n (g/L) is the Freundlich exponent. A plot of $\log q_e$ versus $\log C_e$ used to determine the Freundlich constant and its exponent.

Temkin isotherm: Temkin adsorption isotherm contains a factor that explicitly takes into an account absorbing species adsorbent interactions. It is defined by the following equation,

$$q_e = \frac{R_T}{b} \ln(K_T C_e) \quad (6)$$

The linear form of the above equation is

$$q_e = B_1 \ln K_T + B_1 \ln C_e \quad (7)$$

where $B_1 = RT/b$, KT (L/mg) is the equilibrium binding constant, B_1 is a constant related to the heat of adsorption. A plot of q_e versus $\ln C_e$ enables the determination of isotherm constant B_1 and K_T from the slope and intercepts [39]. The plots for each

isotherm are shown in Fig. 2 and the isotherm parameters are tabulated in Table-1.

From the isotherm graphs and parameters, Langmuir isotherm R_L value is below 1 in all cases which infers that the adsorption is high. In case of correlation value, the Freundlich and Temkin isotherms values are below the Langmuir isotherm. It is evident that in all cases, the Langmuir equation represents the best fit of experimental data than the other isotherms.

Adsorption kinetics: The kinetics of adsorption processes were carried out for the prepared clay/polymer nanocomposites by varying the adsorbate concentrations as 25, 50, 75 and 100 mg/L for malachite green and amido black 10B. The kinetic data for the adsorption of dyes with all the four varying initial concentrations were tested with the kinetic models namely pseudo first-order, pseudo second-order models, intra particle models and Boyd plots.

Pseudo first-order model: The pseudo first-order equation [39,42] is generally expressed as follows:

$$\frac{dq_t}{dt} = k_1 (q_e - q_t) \quad (8)$$

After integrating with the following boundary conditions, $t = 0$ to $t = t$ and $q_t = 0$ to $q_t = q_t$; eqn. 8 becomes

$$q_t = q_e (1 - e^{-k_1 t}) \quad (9)$$

The linear form of eqn. 9 for use in kinetic analysis of data as:

$$\ln(q_e - q_t) = \ln(q_e - k_1 t) \quad (10)$$

where q_e (mg/g) and q_t (mg/g) are the amounts of adsorbate adsorbed at equilibrium and at time t , respectively, and k_1 (min^{-1}) is the rate constant of pseudo first-order adsorption.

Pseudo second-order model: The pseudo second-order chemisorption kinetic rate equation [39,41] is expressed as:

$$\frac{dq_t}{dt} = k_2 (q_e - q_t)^2 \quad (11)$$

On integration eqn. 11 becomes

$$\frac{1}{(q_e - q_t)} = \frac{1}{q_e} + k_2 t \quad (12)$$

The linear form of integrated rate law for the pseudo second order reaction, eqn. 12 becomes as:

$$\frac{t}{q_t} = \frac{1}{k_2 q_e^2} + \frac{1}{q_t} t \quad (13)$$

where k_2 (g/mg min) is the equilibrium rate constant. If the pseudo second-order kinetic equation is applicable, the plot of t/q_t against t should give a linear relationship, from which q_e and k_2 can be determined from the slope and intercept of the plot. The plots for each kinetic model are shown in Figs. 3 an 4 and the kinetic parameters are tabulated in Table-2.

TABLE-1
ISOTHERM PARAMETERS FOR THE ADSORPTION OF MALACHITE GREEN AND
AMIDO BLACK 10B ONTO POLYMER/CLAY NANOCOMPOSITES

Adsorbate	Langmuir				Freundlich			Temkin		
	K_L	q_m (mg/g)	R_L	r^2	K_F ($\text{mg}^{1-1/n}$ $\text{L}^{1/n} \text{g}^{-1}$)	N (g/L)	r^2	B_1	K_T (L/g)	r^2
Malachite green	0.057	34.75	0.0173	0.9958	0.171	0.573	0.9872	1.744	0.364	0.9872
Amido black 10B	0.012	28.8	0.0776	0.9945	2.437	0.742	0.9545	1.348	1.935	0.9455

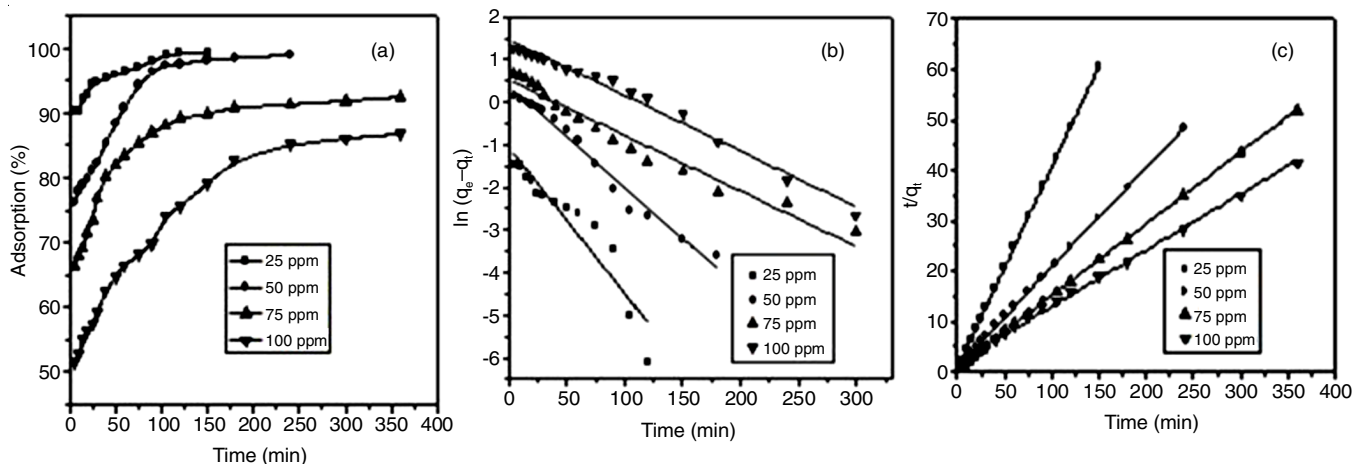


Fig. 3. Plots of adsorption kinetic equations for adsorption of malachite green dye onto clay/polymer nanocomposites (a) Percentage adsorption, (b) pseudo first-order plots, (c) pseudo second-order plots

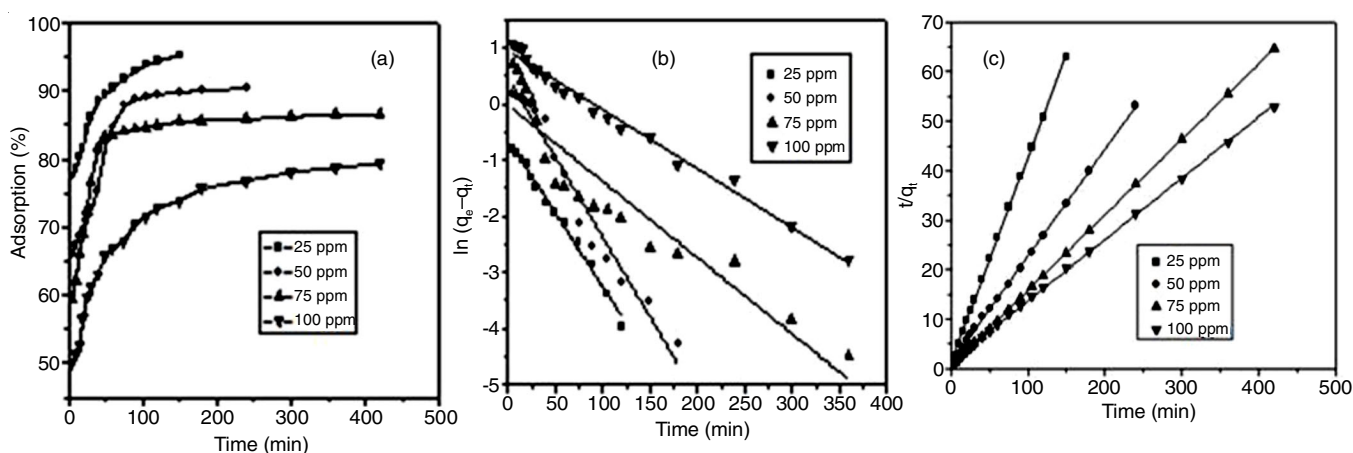


Fig. 4. Plots of adsorption kinetic equations for adsorption of amido black 10B dye onto clay/polymer nanocomposites (a) Percentage adsorption, (b) pseudo first-order plots, (c) pseudo second-order plots

TABLE-2 ADSORPTION KINETICS PARAMETERS FOR THE ADSORPTION OF MALACHITE GREEN AND AMIDO BLACK 10B						
C_0 (mg/L)	Pseudo first-order kinetic equation			Pseudo second-order kinetic equation		
	q_1 (mg/g)	K_1 (1/min) $\times 10^2$	r_1^2	q_2 (mg/g)	K_2 [g/(mg min)] $\times 10^3$	r_2^2
Malachite green						
25	0.353	0.034	0.9876	2.499	0.267	0.9998
50	1.476	0.024	0.9766	5.056	0.039	0.9994
75	1.678	0.013	0.9580	7.028	0.024	0.9998
100	4.324	0.009	0.9382	8.945	0.007	0.9964
Amido black 10B						
25	0.538	0.026	0.9902	2.415	0.129	0.9996
50	1.606	0.021	0.9663	4.644	0.058	0.9991
75	0.976	0.014	0.9623	6.551	0.042	0.9999
100	2.597	0.011	0.9869	8.053	0.012	0.9994

The pseudo first-order constant k_1 increased with the decrease in the dye concentration and also increased with the increase in the impregnation ratios of the adsorbent. From these data, it was clear that the pseudo second-order constant k_2 decreased with the increase in the dye concentration and also increased with the increase in the impregnation ratios of adsorbent.

Thermodynamic studies: The amounts of adsorption of dyes on polymer/clay nanocomposites were measured with various temperatures *viz.* 293, 300 and 313 K, using the following eqns. 19-21 [43,44]:

$$K_d = \frac{q_e}{C_e} \quad (19)$$

$$\Delta G = -RT \ln K_d \quad (20)$$

$$\ln K_d = \frac{\Delta S}{R} - \frac{\Delta H}{RT} \quad (21)$$

The values of ΔH° and ΔS° of different adsorbate adsorption were calculated by fitting the experimental data to eqn. 21 and the value of ΔG° was obtained by using eqn. 20 as shown in Table-3.

TABLE-3
THERMODYNAMIC PARAMETERS OF MALACHITE GREEN AND
AMIDO BLACK 10B ADSORPTION ONTO POLYMER/CLAY NANOCOMPOSITES

Adsorbate	ΔH° (KJ/mol)	ΔS° (KJ/mol)	ΔG° (KJ/mol)		
			293 K	300 K	313 K
Malachite green	130.79	425.49	-12.453	-12.879	-13.304
Amido black 10 B	53.37	146.20	-42.782	-44.244	-45.706

From the above results, it was clear that the adsorption process is spontaneous with the negative values of ΔG° . The positive value of ΔS° shows the increased disorder at the solid and solution interface and it was also observed that the process of adsorption of dyes onto polymer/clay is endothermic in nature due to the positive values of standard enthalpy change ΔH° .

CONFLICT OF INTEREST

The authors declare that there is no conflict of interests regarding the publication of this article.

REFERENCES

- G. Bayramoglu and M.Y. Arica, *J. Hazard. Mater.*, **144**, 449 (2007); <https://doi.org/10.1016/j.jhazmat.2006.10.058>.
- R. Easton, ed.: P. Cooper, *The Dye Maker's View, Colour in Dye House Effluent*, Society of Dyers and Colourists, The Alden Press: Oxford, pp. 9-21 (1995).
- G.S. Heiss, B. Gowan and E.R. Dabbs, *FEMS Microbiol. Lett.*, **99**, 221 (1992); <https://doi.org/10.1111/j.1574-6968.1992.tb05571.x>.
- S.B. Wang and Z.H. Zhu, *J. Hazard. Mater.*, **136**, 946 (2006); <https://doi.org/10.1016/j.jhazmat.2006.01.038>.
- V.K. Gupta, A. Mittal, L. Krishnan and V. Gajbe, *Sep. Purif. Technol.*, **40**, 87 (2004); <https://doi.org/10.1016/j.seppur.2004.01.008>.
- V. Vimonses, S. Lei, B. Jin, C.W.K. Chow and C. Saint, *Appl. Clay Sci.*, **43**, 465 (2009); <https://doi.org/10.1016/j.clay.2008.11.008>.
- V. Meshko, L. Markovska, M. Mincheva and A.E. Rodrigues, *Water Res.*, **35**, 3357 (2001); [https://doi.org/10.1016/S0043-1354\(01\)00056-2](https://doi.org/10.1016/S0043-1354(01)00056-2).
- E. Forgacs, T. Cserháti and G. Oros, *Environ. Int.*, **30**, 953 (2004); <https://doi.org/10.1016/j.envint.2004.02.001>.
- V.K. Garg, R. Kumar and R. Gupta, *Dyes Pigments*, **62**, 1 (2004); <https://doi.org/10.1016/j.dyepig.2003.12.016>.
- K. Kadirvelu, M. Palanival, R. Kalpana and S. Rajeswari, *Bioresour. Technol.*, **74**, 263 (2000); [https://doi.org/10.1016/S0960-8524\(00\)00013-4](https://doi.org/10.1016/S0960-8524(00)00013-4).
- S. Nouri, F. Haghsereshat and G.Q.M. Lu, *Adsorption*, **8**, 215 (2002); <https://doi.org/10.1023/A:1021260501001>.
- M.F.R. Pereira, S.F. Soares, J.J.M. Orfao and J.L. Figueiredo, *Carbon*, **41**, 811 (2003); [https://doi.org/10.1016/S0008-6223\(02\)00406-2](https://doi.org/10.1016/S0008-6223(02)00406-2).
- S.B. Wang and H. Li, *J. Hazard. Mater.*, **126**, 71 (2005); <https://doi.org/10.1016/j.jhazmat.2005.05.049>.
- P. Janos, H. Buchtova and M. Ryznarova, *Water Res.*, **37**, 4938 (2003); <https://doi.org/10.1016/j.watres.2003.08.011>.
- C.C. Wang, L.C. Juang, T.C. Hsu, C.K. Lee, J.F. Lee and F.C. Huang, *J. Colloid Interface Sci.*, **273**, 80 (2004); <https://doi.org/10.1016/j.jcis.2003.12.028>.
- H.B. Bradl, *J. Colloid Interface Sci.*, **277**, 1 (2004); <https://doi.org/10.1016/j.jcis.2004.04.005>.
- H.H. Murray, *Appl. Clay Sci.*, **17**, 207 (2000); [https://doi.org/10.1016/S0169-1317\(00\)00016-8](https://doi.org/10.1016/S0169-1317(00)00016-8).
- P. Liu and L. Zhang, *Sep. Purif. Technol.*, **58**, 32 (2007); <https://doi.org/10.1016/j.seppur.2007.07.007>.
- F. Cadena, R. Rizvi and R.W. Peter, *Feasibility Studies for the Removal of Heavy Metal from Solution Using Tailored Bentonite, Hazardous and Industrial Wastes*, Proceedings of 22nd Mid Atlantic Industrial Waste Conference, Drexel University: Philadelphia, pp 77 (1990).
- R.E. Grim, *Applied Clay Mineralogy*, McGraw-Hill: New York (1962).
- S. Sinha Ray and M. Okamoto, *Prog. Polym. Sci.*, **28**, 1539 (2003); <https://doi.org/10.1016/j.progpolymsci.2003.08.002>.
- H. Fischer, *Mater. Sci. Eng. C*, **23**, 763 (2003); <https://doi.org/10.1016/j.msec.2003.09.148>.
- Q.H. Zeng, A.B. Yu, G.Q. Lu and D.R. Paul, *J. Nanosci. Nanotechnol.*, **5**, 1574 (2005); <https://doi.org/10.1166/jnn.2005.411>.
- A. Gil, L.M. Gandia and M.A. Vicente, *Catal. Rev., Sci. Eng.*, **42**, 145 (2000); <https://doi.org/10.1081/CR-100100261>.
- T. Shichi and K. Takagi, *J. Photochem. Photobiol. Photochem. Rev.*, **1**, 113 (2000); [https://doi.org/10.1016/S1389-5567\(00\)00008-3](https://doi.org/10.1016/S1389-5567(00)00008-3).
- S. Choi and Y. Jeong, *Fibers Polym.*, **9**, 267 (2008); <https://doi.org/10.1007/s12221-008-0042-0>.
- D. Chen, L. Cao, T.L. Hanley and R.A. Caruso, *Adv. Funct. Mater.*, **22**, 1966 (2012); <https://doi.org/10.1002/adfm.201102878>.
- K.J. Yao, M. Song, D.J. Hourston and D.Z. Luo, *Polymer*, **43**, 1017 (2002); [https://doi.org/10.1016/S0032-3861\(01\)00650-4](https://doi.org/10.1016/S0032-3861(01)00650-4).
- M.E.M. Hassouna and M.E.M.A. Hafez, *Int. J. Eng. Res. Gen. Sci.*, **3**, 6 (2015).
- L.A. Utracki, *Eur. Polym. J.*, **45**, 1891 (2009); <https://doi.org/10.1016/j.eurpolymj.2009.04.009>.
- A. Usuki, A. Tukigase and M. Kato, *Polymer*, **43**, 2185 (2002); [https://doi.org/10.1016/S0032-3861\(02\)00013-7](https://doi.org/10.1016/S0032-3861(02)00013-7).
- J.H. Wu and M.M. Lerner, *Chem. Mater.*, **5**, 835 (1993); <https://doi.org/10.1021/cm00030a019>.
- S.K. Modak, A. Mandal and D. Chakrabarty, *Polym. Compos.*, **34**, 32 (2013); <https://doi.org/10.1002/pc.22374>.
- I.D. Mall, V.C. Srivastava, G.V.A. Kumar and I.M. Mishra, *Colloids Surf. A Physicochem. Eng. Asp.*, **278**, 175 (2006); <https://doi.org/10.1016/j.colsurfa.2005.12.017>.
- M. Özacar and I.A. Sengil, *J. Hazard. Mater.*, **98**, 211 (2003); [https://doi.org/10.1016/S0304-3894\(02\)00358-8](https://doi.org/10.1016/S0304-3894(02)00358-8).
- C. Namasivayam, N. Muniasamy, K. Gayatri, M. Rani and K. Ranganathan, *Bioresour. Technol.*, **57**, 37 (1996); [https://doi.org/10.1016/0960-8524\(96\)00044-2](https://doi.org/10.1016/0960-8524(96)00044-2).
- M. Ozacar and I.A. Sengil, *Environ. Geol.*, **45**, 762 (2004); <https://doi.org/10.1007/s00254-003-0936-5>.
- I. Langmuir, *J. Am. Chem. Soc.*, **40**, 1361 (1918); <https://doi.org/10.1021/ja02242a004>.
- G. Crini, H.N. Peindy, F. Gimbert and C. Robert, *Separ. Purif. Technol.*, **53**, 97 (2007); <https://doi.org/10.1016/j.seppur.2006.06.018>.
- H. Freundlich, *Z. Phys. Chem.*, **57U**, 385 (1907); <https://doi.org/10.1515/zpch-1907-5723>.
- C. Gerente, V.K.C. Lee, P.L. Cloirec and G. McKay, *Crit. Rev. Environ. Sci. Technol.*, **37**, 41 (2007); <https://doi.org/10.1080/10643380600729089>.
- S. Arivoli, Ph.D. Thesis, Kinetic and Thermodynamic Studies on the Adsorption of Some Metal Ions and Dyes onto Low Cost Activated Carbons, Gandhigram Rural University, Gandhigram, India (2007).
- S. Arivoli and M. Hema, *Int. J. Phys. Sci.*, **2**, 10 (2007).
- S. Arivoli, K. Kalpana, R. Sudha and T. Rajachandrasekar, *E-J. Chem.*, **238** (2007); <https://doi.org/10.1155/2007/304305>.